Supplementary Information to:

High Surface Area Mixed Lanthanum Nickelate/Ferrates ($LaNi_{1-x}Fe_xO_3$) via Modified Carbon Templating Coated on Nickel in Alkaline OER

Nikolas Mao Kubo[a], Harol Moreno Fernández[b], Ilias Efthimiopoulos[c], Leila Novalic[a], Martin Rabe[c], Jan P. Hofmann[b], and Regina Palkovits*[a,d]

[a] N. M. Kubo, L. Novalic, Prof. R. Palkovits
Institute of Technical and Macromolecular Chemistry
RWTH Aachen University
Worringerweg 2, 52074 Aachen, Germany
E-mail: palkovits@itmc.rwth-aachen.de

[b] Dr. H. Moreno Fernández, Prof. Dr. J. P. Hofmann
Surface Science Laboratory, Department of Materials and Geosciences, Surface Science Laboratory
Technical University of Darmstadt
Peter-Grünberg-Straße 4, 64287 Darmstadt, Germany

[c] Dr. I. Efthimiopoulos, Dr. M Rabe
Department Interface Chemistry and Surface Engineering
Max-Planck-Institut für Nachhaltige Materialien
Max-Planck-Straße 1, 40237 Düsseldorf, Germany

[d] Prof. Dr. R. Palkovits
Institute for a Sustainable Hydrogen Economy (INW-2)
Forschungszentrum Jülich
Marie-Curie-Straße 5, 52428 Jülich, Germany

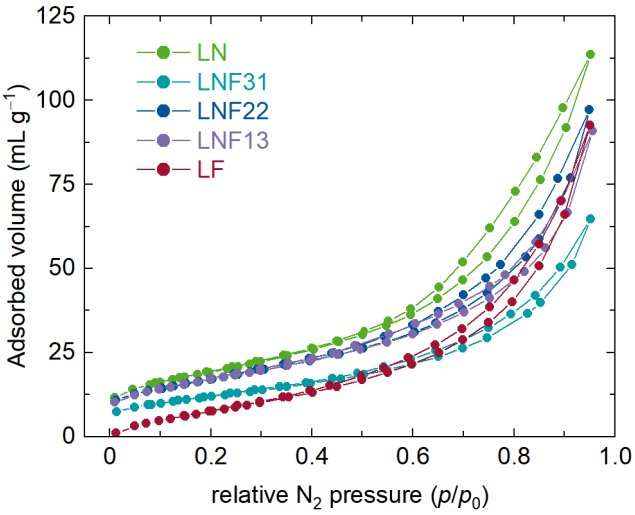

Figure S1. N_2 physisorption isotherms of all powdered $LaNi_{1-x}Fe_xO_3$ perovskite samples.

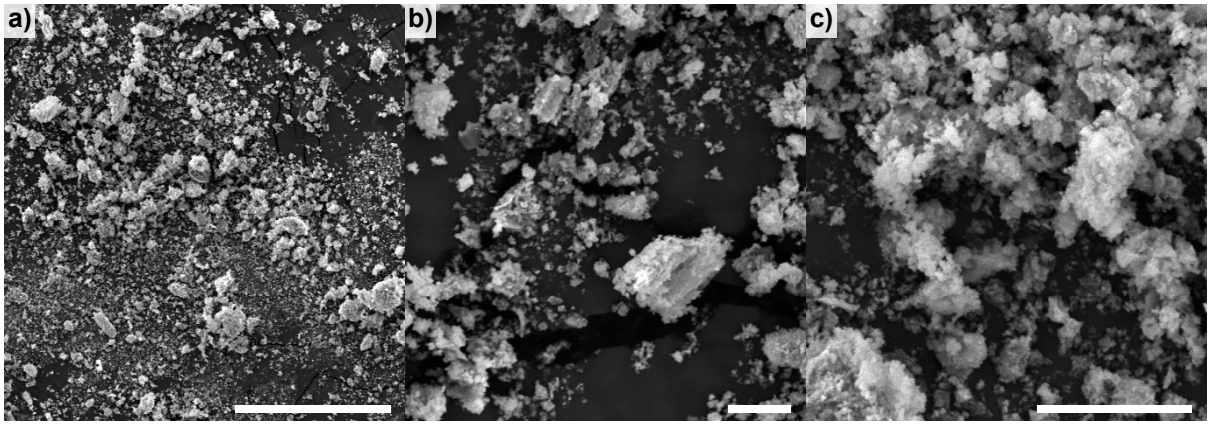

Figure S2. SEM images of $LaNiO_3$ (LN) in powder form. Scale bars: a) 100 µm, b) 10 µm, and c) 10 µm.

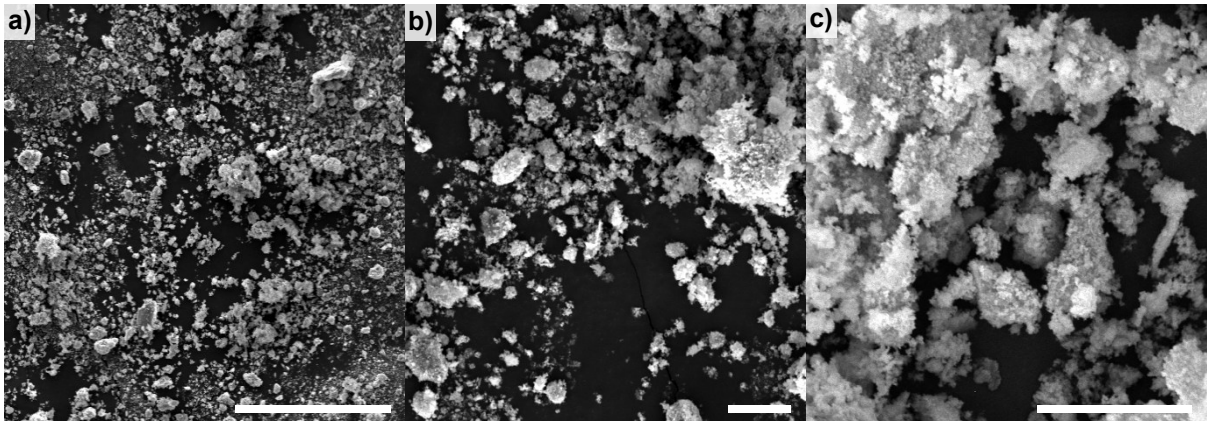

Figure S3. SEM images of LNF31 in powder form. Scale bars: a) 100 µm, b) 10 µm, and c) 10 µm.

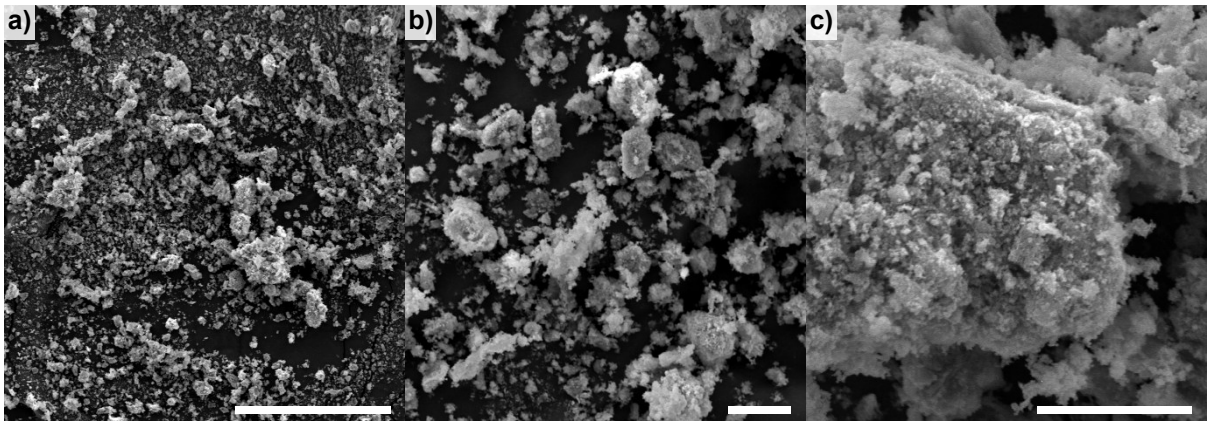

Figure S4. SEM images of LNF22 in powder form. Scale bars: a) 100 μm, b) 10 μm, and c) 10 μm.

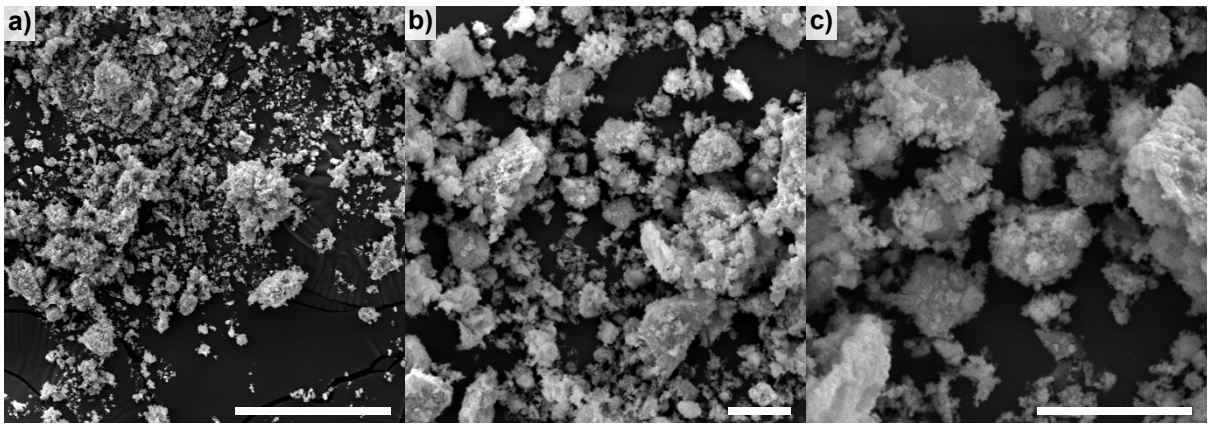

Figure S5. SEM images of LNF13 in powder form. Scale bars: a) 100 μm, b) 10 μm, and c) 10 μm.

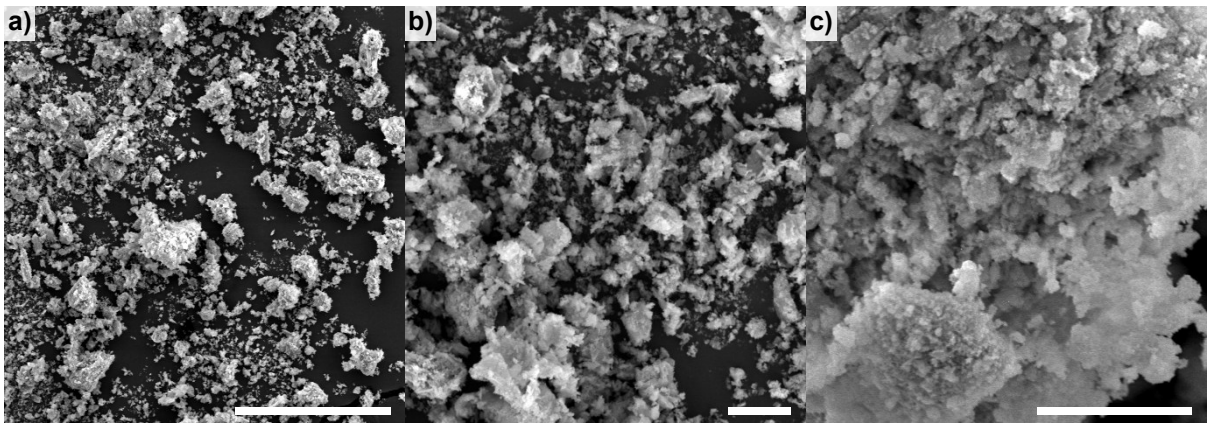

Figure S6. SEM images of LF ($LaFeO_3$) in powder form. Scale bars: a) 100 μm, b) 10 μm, and c) 10 μm.

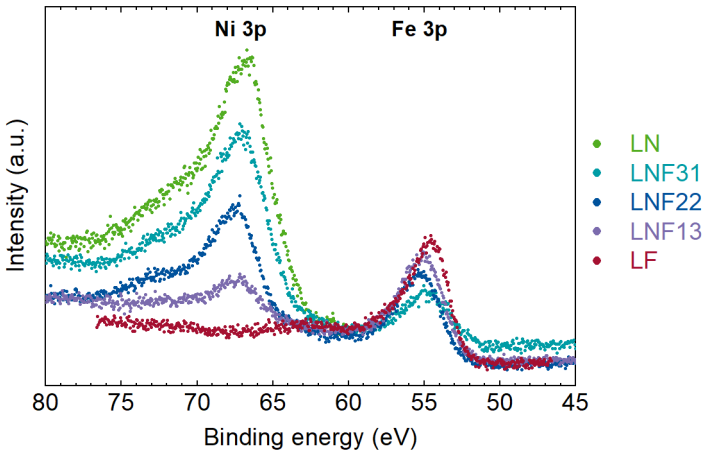

Figure S7. XPS binding energies of Ni 3p and Fe 3p core level spectra of all powder $LaNi_{1-x}Fe_xO_3$ powder samples, showing the consistent decrease of the Ni 3p peak and increase of the Fe 3p peak with increasing *x*.

Table S1. Fractions of Ni and Fe in $LaNi_{1-x}Fe_xO_3$ powder samples in atomic percent calculated using the Casa XPS software.

Sample	Ni (at. %)	Fe (at. %)
LN	100	0
LNF31	80	20
LNF22	63	37
LNF13	30	70
LF	5	95

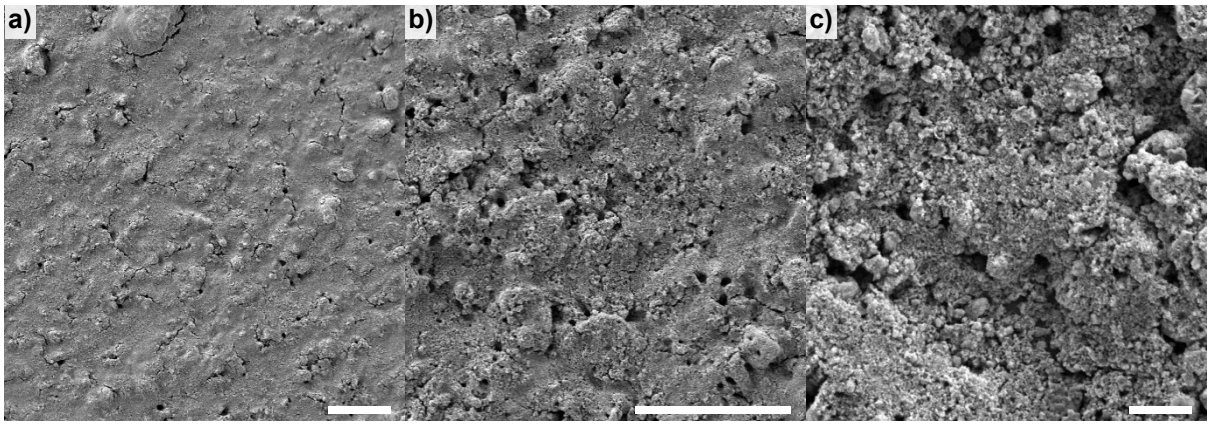

Figure S8. SEM images of Ni substrate coated with 1 mg cm^{-2} LN, heated in stagnant air at 400°C for 1 h (10 K min^{-1}). Scale bars: a) 100 µm, b) 100 µm, and c) 10 µm.

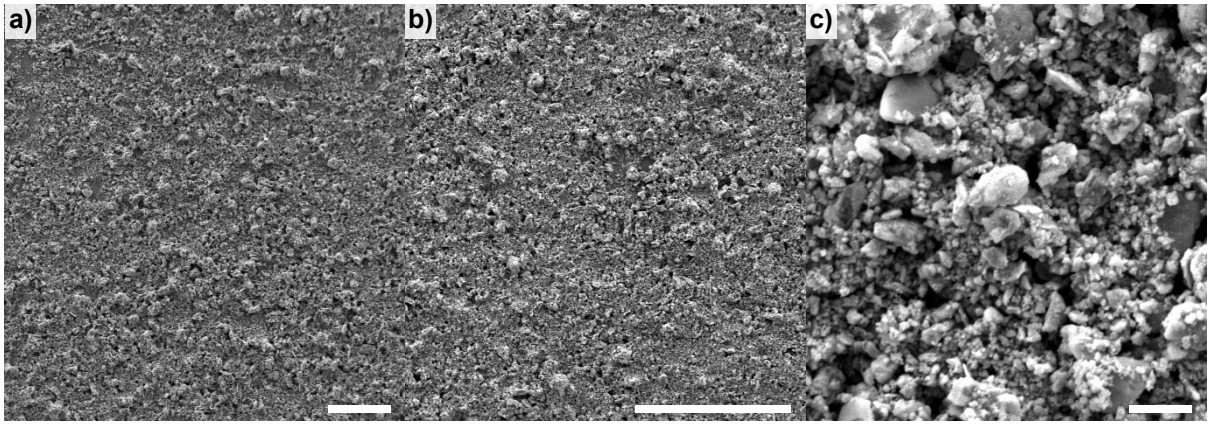

Figure S9. SEM images of Ni substrate coated with 1 mg cm^{-2} LF, heated in stagnant air at 400°C for 1 h (10 K min^{-1}). Scale bars: a) 100 µm, b) 100 µm, and c) 10 µm.

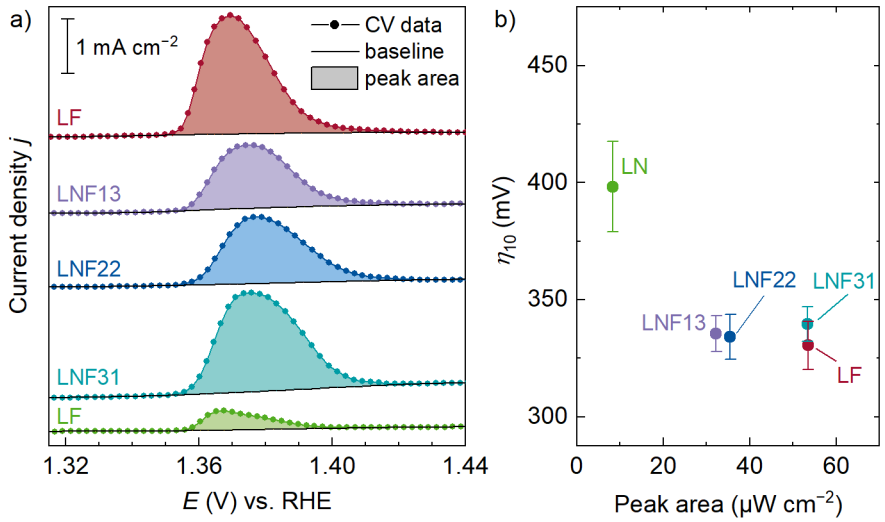

Figure S10. a) Ni(II)/Ni(III) oxidation peak area in one representative CV forward scan per $LaNi_{1-x}Fe_xO_3$ sample recorded at a scan rate of 5 mV s^{-1} in 1 M KOH electrolyte. b) correlation of overpotential η_{10} determined at a current density of 10 mA cm^{-2} during the CV forward scans, averaged over triplicate measurements and the peak areas of the corresponding Ni(II)/Ni(III) peaks.

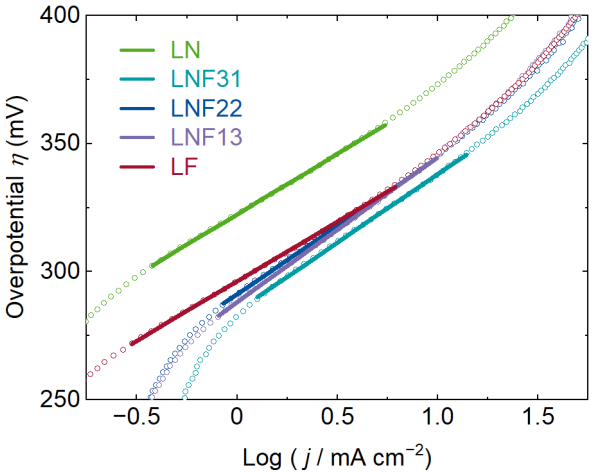

Figure S11. Tafel plots of the representative iR drop-corrected CV forward scans (dotted lines) measured in 1 M KOH at a scan rate of 5 mV s^{-1} as shown in Fig. 5. The solid lines represent the linear regressions applied for the determination of the Tafel slopes in the corresponding potential windows where a linear relation between log *j* and the overpotential *η* is observed for each sample.

Table S2. Tafel slopes determined from the linear regressions in the Tafel plots of the representative iR-corrected CV forward scans presented in Figure S11, following the Tafel equation $\eta = a + b \times \log j$.

Sample	Tafel slope (mV dec^{-1})
LN	47
LNF31	53
LNF22	53
LNF13	56
LF	47

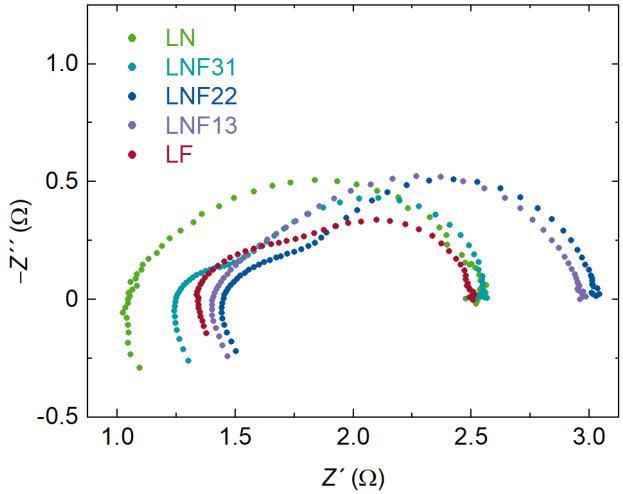

Figure S12. Nyquist plots of the impedance spectra recorded from all $LaNi_{1-x}Fe_xO_3$ perovskite samples at an applied potential of 1.6 V vs. RHE with a root mean square (RMS) potential amplitude of 10 mV for 10 frequencies per decade between 100 kHz and 0.1 Hz. The uncompensated resistances R_u can be estimated from the left *x*-axis intercept of the semicircles and are applied for iR-correction of the potentials.[1] The charge transfer resistances can be estimated as the widths of the respective semicircles and can give quantitative insight into the activation barrier of the corresponding electrode.[1] The charge transfer resistances mostly follow the trend of the activities of the substrates.

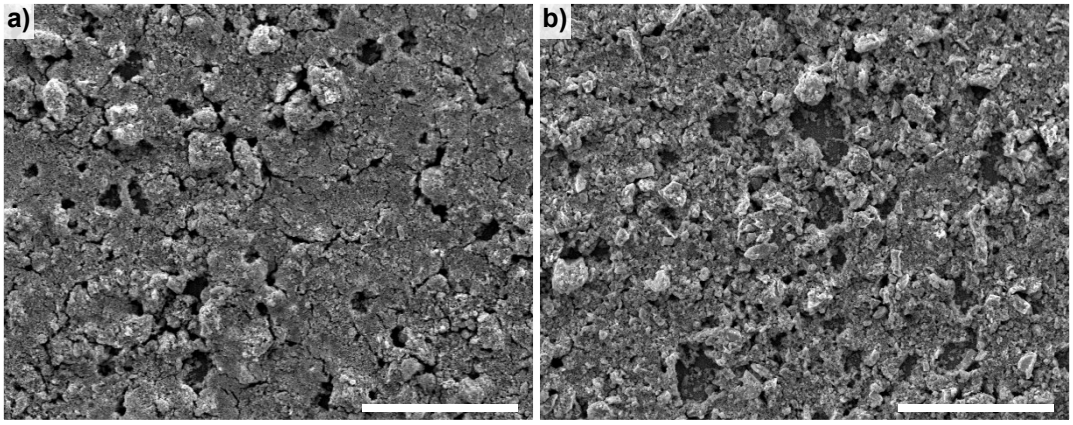

Figure S13. SEM images of Ni substrate coated with 1 mg cm^{-2} of a) LN and b) LF after additional tempering for 3 h at 700°C (10 K min^{-1}) in a N_2 atmosphere before chronopotentiometry measurements. Scale bars: 100 µm.

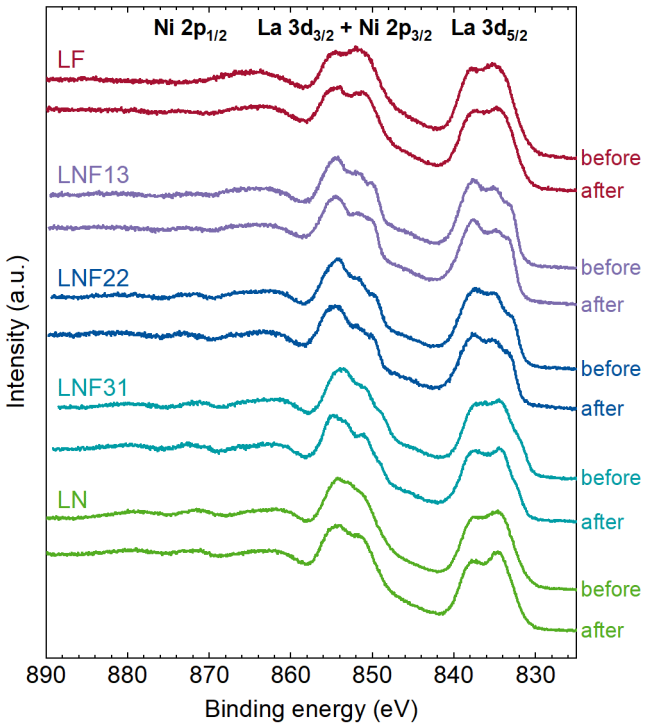

Figure S14. XPS binding energies of La 3d and Ni 2p core level spectra of all $LaNi_{1-x}Fe_xO_3$ samples coated as catalysts on Ni substrates before and after 24 h of galvanostatic chronopotentiometry at 10 mA cm^{-2} in 1 M KOH electrolyte, interrupted every 4 h.

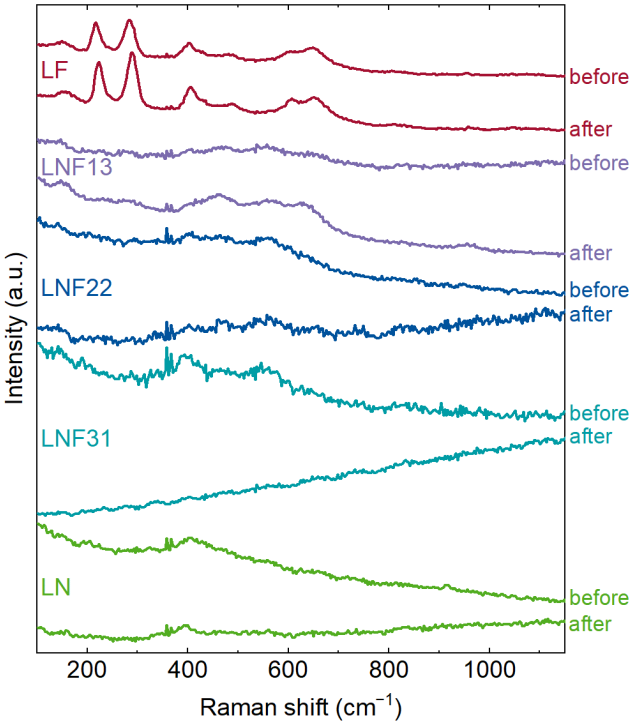

Figure S15. Raman spectra of all $LaNi_{1-x}Fe_xO_3$ samples coated as catalysts on Ni substrates before and after 24 h of galvanostatic chronopotentiometry at 10 mA cm^{-2} in 1 M KOH electrolyte, interrupted every 4 h.

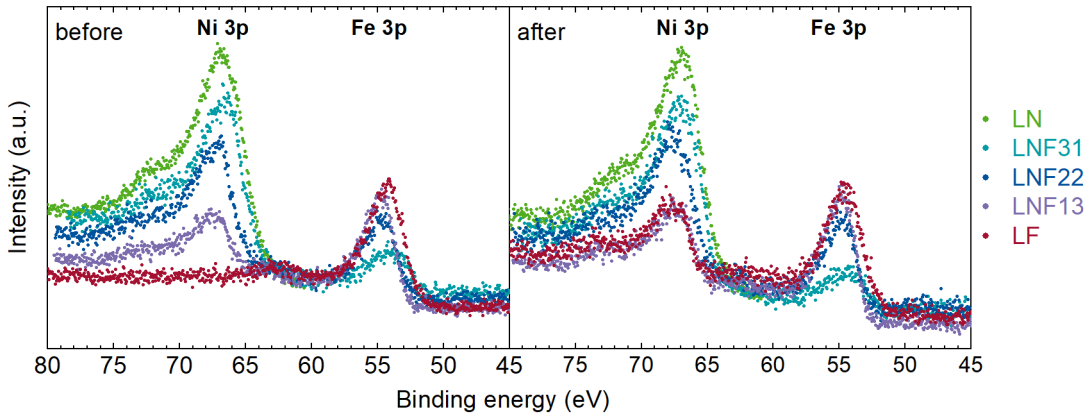

Figure S16. XPS binding energies of Ni 3p and Fe 3p core level spectra of all $LaNi_{1-x}Fe_xO_3$ samples coated as catalysts on Ni substrates before and after 24 h of galvanostatic chronopotentiometry (CP) at 10 mA cm^{-2} in 1 M KOH, interrupted every 4 h.

Table S3. Fractions of Ni and Fe in $LaNi_{1-x}Fe_xO_3$ samples coated as catalysts on Ni substrate before and after 24 h of CP at 10 mA cm^{-2} in atomic percent calculated from the integrated peak areas of the Ni 3p and Fe 3p signals shown in Figure S13.

Sample	before		after	
	Ni (at. %)	Fe (at. %)	Ni (at.%)	Fe (at. %)
LN	100	0	100	0
LNF31	80	20	82	18
LNF22	65	35	65	35
LNF13	40	60	46	54
LF	7	93	58	42

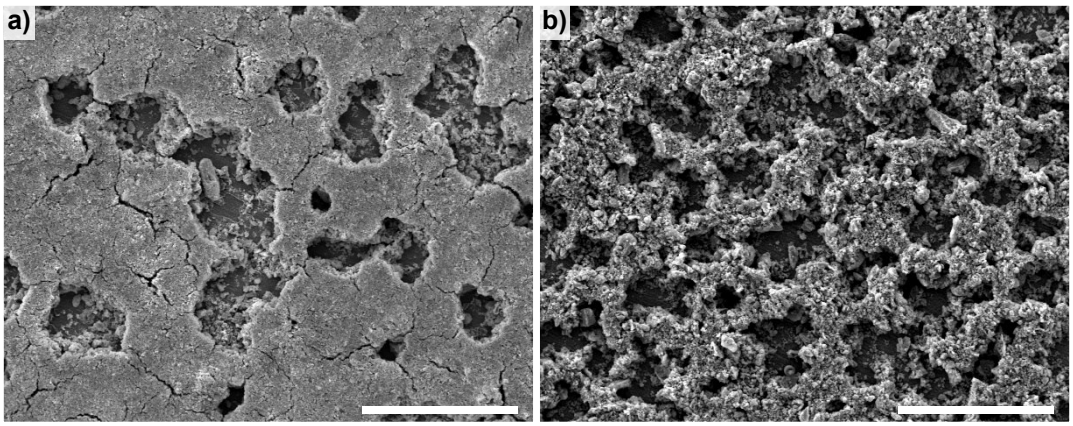

Figure S17. SEM images of Ni substrate coated with 1 mg cm^{-2} of a) LN and b) LF after 24 h of galvanostatic chronopotentiometry at 10 mA cm^{-2} in 1 M KOH electrolyte. Scale bars: 100 µm.

References:

[1] A. J. Bard, L. R. Faulkner. *Electrochemical Methods – Fundamentals and Applications*; John Wiley & Sons, **2001**, p .386.